



# Use of *Ricinus communis* shredded material as filler in rotational molded parts to improve the bio-disintegration behavior

Francisco Romero<sup>1</sup> · Zaida Ortega<sup>2</sup> · Jessica Castellano<sup>1</sup> · Antonio N. Benítez<sup>2</sup> · María Dolores Marrero<sup>1</sup> · Luis Suárez<sup>1</sup>

Received: 24 June 2022 / Revised: 10 August 2022 / Accepted: 18 November 2022 /  
Published online: 30 November 2022  
© The Author(s) 2022

## Abstract

This paper focuses on the use of castor oil plant (*Ricinus communis*) as filler in rotomolded parts using polyethylene (PE) and polylactic acid (PLA) as polymer matrixes. The vegetable shredded material was used in 5 and 10% weight following a dry blending procedure and then rotomolded to obtain cube test parts. This material was characterized to determine its chemical composition, thermal stability, and structure. The NaOH-treated material shows reduced hemicellulose content and higher thermal stability. Obtained composite materials were characterized in terms of mechanical (tensile, flexural, and impact) and thermal properties, morphology, and bio-disintegration behavior. The use of *Ricinus* as filler in rotomolded PE composite decreases, in general terms, mechanical properties of neat PE, while no significant changes in thermal or bio-disintegration properties are found. On the contrary, PLA composites show higher tensile strength and similar Young's modulus than the matrix, although with reduced flexural and impact properties. Alkali-treated *Ricinus* material produces parts with higher porosity and thus, lower mechanical properties than composites with untreated material. Finally, the incorporation of this vegetal material modifies to a great extent the thermal properties of the PLA matrix. The bio-disintegration rate increases due to the use of fibers, probably because of the higher moisture absorption of composites.

**Keywords** Castor oil plant · *Ricinus communis* · Rotational molding · Characterization · Disintegration · PLA · PE

---

✉ Zaida Ortega  
zaida.ortega@ulpgc.es

<sup>1</sup> Departamento de Ingeniería Mecánica, Universidad de Las Palmas de Gran Canaria, 35017 Las Palmas, Spain

<sup>2</sup> Departamento de Ingeniería de Procesos, Universidad de Las Palmas de Gran Canaria, 35017 Las Palmas, Spain

## Introduction

Rotational molding is a well-established technology, mainly used in producing hollow parts with good surface quality and mechanical properties, with almost no internal stresses. One of the main limitations of this technology is that the range of available materials is not as comprehensive as for other polymer processing technologies (in fact, polyethylene (PE) accounts for more than 90% of the rotomolding market [1]). This lack of alternatives is even more critical when considering the environmental behavior of obtained parts. The impact of polymers on the environment is out of any discussion currently. In recent years, biodegradable polymers have become more prevalent in consumer products to overcome this problem.

For this reason, several authors have focused on using new materials adapted to rotomolding specificities. Polylactic acid (PLA) is one of the most studied alternatives [2–6] due to its recyclability, good mechanical properties, and biodegradability under certain conditions. In order to improve the process sustainability, some authors have proposed using recycled materials from post-consumer plastics [7] or recycled PLA fractions [8]. Other authors have also suggested introducing natural fibers to improve rotomolded parts' properties. For example, flax [9], cabuya, and sisal [10] or agave [11] have been introduced in proportions of up to 10% (in weight) in PE and PLA matrixes, being this loading commonly used in rotomolding [12]. Higher loadings are not typical due to reduced mechanical properties, mainly due to increased voids content and the poor adhesion between the fibers and the polymer matrix. Other authors have increased this proportion, reaching up to 30% [1, 13] drastic decreases in mechanical behavior. An appropriate selection of particle size distribution [14–16] or using compatibilizers [6, 17] could reduce this effect. In the last years, with the rise of sustainability concerns and the need to increase the use of resources, several authors have moved on to using alternative raw materials to be used as reinforcement or fillers of composite materials. For example, Ortega et al. produced composites with 5% w/w of banana and abaca fibers with significant improvements in mechanical properties, except for impact strength [18], while Hejna et al. obtained composites with up to 20% w/w of wheat bran, although only those with up to 5% content did not show significant loss of mechanical properties [1]. Buckwheat husk, reed, or bamboo are other materials proposed to broaden the options of using lignocellulosic materials [13, 16, 19, 20]. Other authors introduced in rotomolded parts some fillers traditionally considered waste materials, such as cable covers [21] or copper slag from mining [2].

In this sense, the *Ricinus communis* or castor bean plant is an interesting source of lignocellulosic material. This plant is commercially grown to produce castor oil. This product has a wide range of applications, from pharmaceutical products to lubricants. One of such uses is the formulation of polymers, especially polyamide (PA11, commercially known as Rilsan, from Arkema). However, the seeds for oil obtaining are only a small fraction of the plant, so some works about using *Ricinus* by-products have been performed. For example, the cake from oil extraction can be used to obtain a biopolymer based on proteins [22] or as filler for a PE/PHB composite [23].

Regarding the use of fibers from this plant, some authors have already proposed the extraction of fibers with textile quality from the outer bark of the stems [24]. Other studies have used the internal parts of the stems after a retting process to obtain fibers, which were later used as reinforcement of polyester [25] or epoxy composites [26–29]. Finally, Heitzmann and collaborators have proposed using this PA11 combined with bast fibers from the stems [22].

This paper focuses on the study of the potential use of material from *Ricinus communis* stems as filler for rotomolded parts, starting with the characterization of the vegetal material. PE and PLA matrixes are used to obtain composite materials with the milled stems, characterizing the produced parts. Special attention is paid to the composites' bio-disintegration properties based on PLA to determine the cellulosic fibers' influence on the polymer matrix's disintegration.

## Materials and methods

### Materials

A general-purpose PE from Matrix in powder form (Revolve N-461, Northampton, UK) was used as one of the matrixes. The polylactic acid (PLA) matrix used was from Corbion (Luminy L105; 99% L-isomer), also in powder form.

*Ricinus communis* particles, under 500  $\mu\text{m}$ , were obtained by milling the stems of the plants in a Retsch ZM 200 mill. The vegetal material was treated with a NaOH 1 N solution at room temperature for 1 h, then neutralized with acetic acid and washed with deionized water. Consequently, untreated and treated vegetal material was characterized and later used for composites production.

All reagents used in *Ricinus* characterization were of analytical grade, purchased from Sigma-Aldrich, and used without further modifications.

### Methods

#### *Ricinus communis* characterization

The particle size distribution was obtained by sieving the milled *Ricinus* in an AS 200 Control device from Retsch. The moisture, ashes, cellulose, hemicellulose, and lignin contents were determined, following standard procedures. Klason lignin was obtained according to ANSI/ASTM 1997a standard [30], while for holocellulose (cellulose and hemicellulose), a gravimetric method was used [31]. Cellulose content was calculated under ANSI/ASTM 1977b standard [32], and hemicellulose content was the difference between holocellulose and cellulose. These assays were performed on ten different samples, with five replicas per sample.

The thermogravimetric analyses were conducted in a MettlerToledo TGA/DSC 1 device, performing a dynamic assay from 25 to 1100 °C at a heating rate of 5 °C/min under a nitrogen atmosphere, with five replicas for each sample (untreated and treated material).

The modifications aroused from the treatment of the samples were also assessed by infrared spectroscopy. FTIR spectra were recorded in a PerkinElmer Spectrum Two spectrophotometer under the attenuated total reflectance (ATR) mode. Each spectrum consists of an average of 64 scans, performed from 4000 to 500  $\text{cm}^{-1}$ , at a resolution of 4  $\text{cm}^{-1}$ .

The material's structure was observed in a scanning electron microscope (SEM) from Hitachi (TM3030 tabletop), working at 15 kV, after sputtering in an SC 760 apparatus from Quorum Technologies for 120 s and 18 mA under an argon atmosphere.

Three replicas from three different batches were used for all these tests. Results are expressed as average values  $\pm$  standard deviations.

### Composites production

The composites were prepared by dry blending the matrix with the fibers (at 5 and 10% weight for PE and 10% weight for PLA) and then, introduced into a lab-made rotomolding device [16]. This has a rotation rate of 2.30 rpm on the primary axis and 9.14 rpm on the secondary axis. Cubic parts of 120 mm side and around 4 mm thickness were obtained, monitoring the temperature inside the mold during the process. After cooling and observation for fiber distribution and possible defects detection, test bars were machined from the cube sides, following standard protocols (ISO 3167:2014 for tensile, ISO 178:2019 for flexural, and ISO 180:2019 for Izod-impact tests).

A good filler distribution is observed (Fig. 1), although with some clustering for 10% loaded composites. The composites with treated *Ricinus* also led to thicker walls due to the formation of clusters and voids appearing. In any case, the inner surface of the parts shows an acceptable quality, with no excessive number of voids or fiber balls inside the mold (not integrated into the part), as pointed out in other papers [33]. Darker color and intense smell are obtained for untreated material parts, which means that NaOH treatment is needed in this case to increase the thermal stability (as also observed from TGA analysis).

### Mechanical testing

The composite specimens' tensile properties (elastic modulus and ultimate tensile strength) were determined following ISO 527-2:2012, at a rate of 10 mm/min. The flexural modulus and strength were measured according to ISO 178:2019, also at 10 mm/min, using a support span of 64 mm. Tensile and flexural tests were performed in an LY-1065 universal testing machine from Dongguan Liyi Test Equipment Co. Ltd. Impact tests were performed on unnotched samples, following ISO 180:2019, using a 5.5 J pendulum and an impact rate of 3.5 m/s in an LY-XJJD 50 from Dongguan Liyi Test Equipment Co. Ltd.

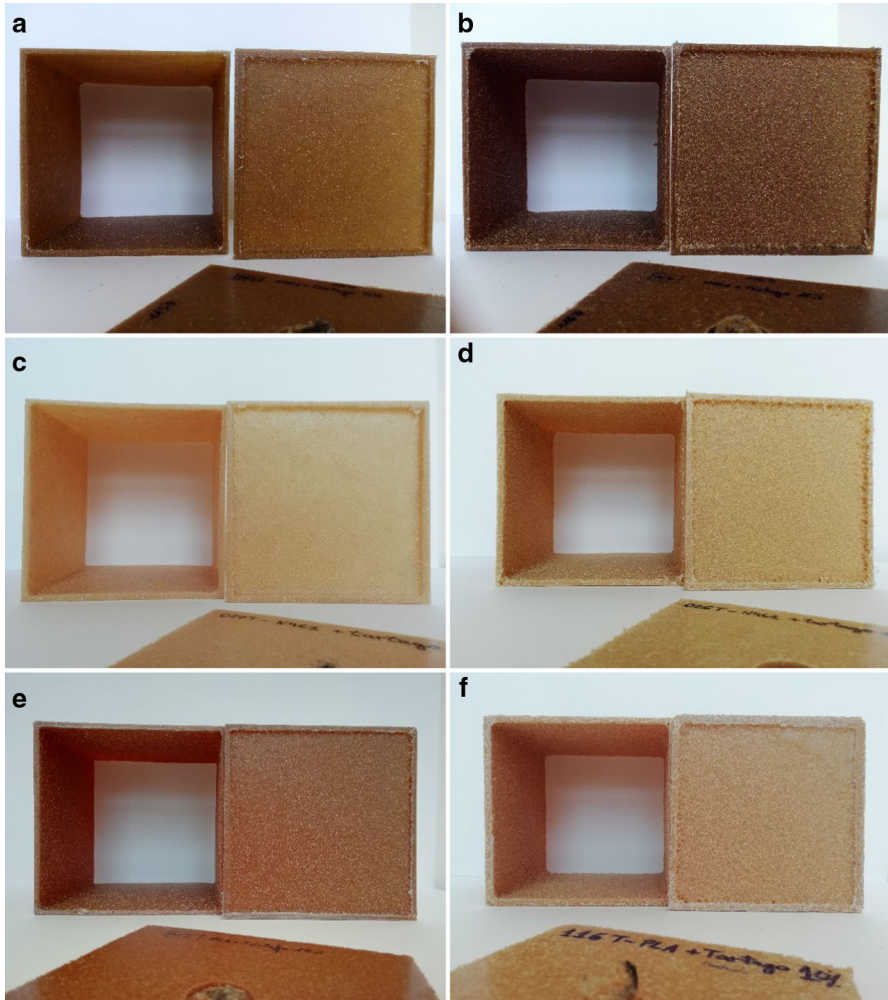


**Fig. 1** Pictures of rotomolded composites (% in weight of lignocellulosic material): **a** 5% *Ricinus*—PE, **b** 10% *Ricinus*—PE, **c** 5% treated *Ricinus*—PE, **d** 10% treated *Ricinus*—PE, **e** 10% *Ricinus*—PLA, and **f** 10% treated *Ricinus*—PLA

### Bio-disintegration assays

Plastic biodegradation is greatly affected by the nature of the material, the type of organism involved in the process, and the conditions in which the process takes place [34]. Disintegrability of the materials was determined by an assay performed in simulated composting conditions, as established in EN-ISO 16929:2021. A synthetic biowaste was prepared by mixing vegetal residues, rabbit feed (commercial product based on alfalfa and vegetable flours), mature compost, wood chips as volumizer agent, urea, and water (up to 55% of the final

weight). This biowaste was placed in boxes (45 × 62 × 18 cm) with holes on the lower part and the sides. A 5 cm layer of expanded clay is placed on the bottom of the boxes to ensure appropriate ventilation and drainage. This biowaste is prepared 48 h before the beginning of the assay.

Once dried and weighted, each sample was buried in the synthetic waste at enough distance not to touch either the box's walls or another piece. The boxes were manually aerated weekly for the first four weeks and then every two weeks. The pH, weight, and humidity levels were assessed weekly during the entire process, checking temperatures daily. The overall duration of the assay was 12 weeks. At the end of the test, the parts were recovered, washed with water, and oven-dried at 105 °C. One could obtain the degree of disintegration from the weight of the samples before and after the assay.

Bio-disintegration behavior was assessed for the neat matrixes and composites with 10% fibers, using 3 replicas per material.

### Microscopic observations

Optical microscopy was performed in an Olympus BX51 microscope to assess visible differences in the surfaces of the parts due to the disintegration process. This microscope also allowed observing the fiber distribution inside the matrix.

SEM analysis was also performed (after sputtering), observing the breaking section of the tensile bars to determine fiber-matrix bonding. The surface of the test bars was also observed before and after the disintegration assay.

### Thermal behavior

Differential scanning calorimetry (DSC) was performed on the samples with 10% filler in a PerkinElmer DSC 4000 apparatus. Measurements were performed at 10 °C/min, from 30 to 200 °C, with two heating cycles. Melting temperature for both heatings ( $T_{m1}$  and  $T_{m2}$ , respectively) was determined, together with crystallization temperature ( $T_c$ ) from the cooling step. Glass transition temperature ( $T_g$ ) was also calculated for PLA samples. Cold crystallization was not observed from any tested formulations, probably due to their high crystallinity levels. Melting and crystallization enthalpies ( $\Delta H_{m1}$ ,  $\Delta H_{m2}$ , and  $\Delta H_c$ ) were also obtained and used for crystallinity degree calculation, using the following expression:

$$\chi = \frac{1}{1 - m_f} \cdot \frac{\Delta H_m}{\Delta H_0} \cdot 100$$

where  $\Delta H_0$  is the enthalpy for 100% crystalline sample (93.7 J/g for PLA and 293 J/g for PE) [13], and  $m_f$  is the mass fraction of the fiber (10% for composites). Three assays were performed for each sample, giving average values and standard deviation results.

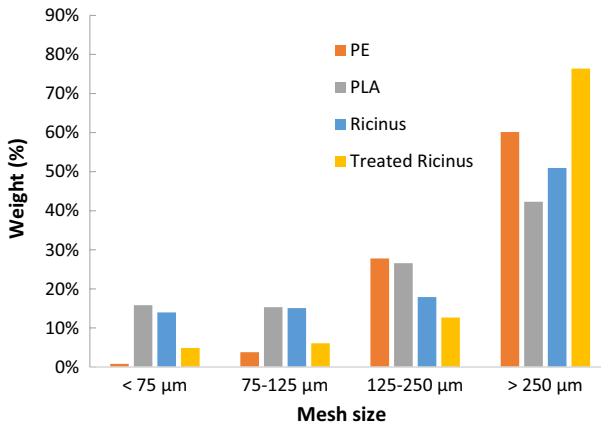


**Fig. 2** Particle size distribution for the materials used: *Ricinus*, treated *Ricinus*, PE, and PLA

**Table 1** Composition (in %) of *Ricinus* and treated *Ricinus* (average values ± standard deviation)

	Cellulose	Hemicellulose	Klason lignin
Shredded material	36.27 ± 1.28	36.80 ± 1.81	22.75 ± 0.75
Treated material	52.21 ± 2.01	19.27 ± 1.96	25.29 ± 1.33

### Infrared spectroscopy (FTIR)

Fourier infrared spectra of the samples were recorded in the range of 500–4000 cm<sup>-1</sup> in a PerkinElmer Spectrum Two spectrometer, in the attenuated total reflection mode (ATR), with a resolution of 4 cm<sup>-1</sup>. Different intensity ratios were calculated for each polymer matrix to determine the extension of the sample changes. Three spectra were obtained for each sample, accumulating 64 scans per spectrum.

## Results and discussion

### *Ricinus communis* characterization

Hanana and Rodrigue et al. [15] have found that the filler’s particle size is determinant for the mechanical behavior of the final composite, obtaining better mechanical results for maple particles of 355–500 μm. Figure 2 shows the particle size distribution of *Ricinus*, PE, and PLA powders. The *Ricinus* particles used in this research have similar size distribution to the PE and PLA powders used in this study and are in the range of what is proposed by these researchers.

Table 1 shows the average values for *Ricinus communis* samples composition. Proteins content was almost null (following the Kjeldahl method; data not shown). The composition of shredded material is similar to this found in other studies [24, 35, 36]. As expected, hemicellulose content decreases due to the NaOH treatment.

Treated material shows a relatively high cellulose content, in the jute or sisal fibers range. Ashes content for shredded material was  $7.76 \pm 0.10\%$ . The woody nature of the plant explains the relatively high content of lignin in the samples.

Figure 3 shows the average recorded spectra for the samples of shredded material before and after the NaOH treatment. The typical bands for lignocellulosic materials can be observed: a broad band at  $3000\text{--}3600\text{ cm}^{-1}$  (O–H stretching), a peak at around  $2900\text{ cm}^{-1}$ , related to C–H aliphatic groups in hemicellulose [37], peak at  $1730\text{ cm}^{-1}$ , (C=O stretching in lignin and hemicellulose [38, 39]) and an intense peak at  $1028\text{ cm}^{-1}$  (C=O stretching ring vibration in cellulose). The second peak shows lower intensity for the treated fibers, indicating the reduced hemicellulose content, as also found in the chemical analysis. The bands at  $1730\text{ cm}^{-1}$  and  $1620\text{ cm}^{-1}$  also decrease due to the NaOH treatment; these bands are related to lower hemicellulose and humidity contents. Finally, the definition of an inflection at  $1100\text{ cm}^{-1}$  may be correlated with the higher amount of cellulose I in the treated fibers [40].

TGA curves for all considered materials show a similar course (Fig. 4), although displaced to higher values for treated samples, especially for the initial decomposition (left limit temperature) (Table 2).

The most important peak found in derivative (DTG) curves is related to cellulose degradation, located at  $333\text{ }^{\circ}\text{C}$  for both types of samples. DTG curves for untreated material show a shoulder at around  $290\text{ }^{\circ}\text{C}$  (Fig. 4), related to the hemicellulose degradation (hemicellulose pyrolysis starts at about  $220\text{ }^{\circ}\text{C}$  [38]). If considering hemicellulose and cellulose pyrolysis ranges ( $210\text{--}315\text{ }^{\circ}\text{C}$  and  $315\text{--}400\text{ }^{\circ}\text{C}$ , respectively), shredded material shows a weight loss of  $27.4\%$  in the first step and  $25.2\%$  in the second one, being the first decrease considerably lower for treated samples ( $1.9\%$ ). In contrast, the  $\alpha$ -cellulose-related step shows higher values ( $53.4\%$ ), which again confirms the modifications performed by the NaOH treatment. The *Ricinus* samples in this work offer similar thermal stability to other commonly used vegetal fibers, such as flax or jute [41].

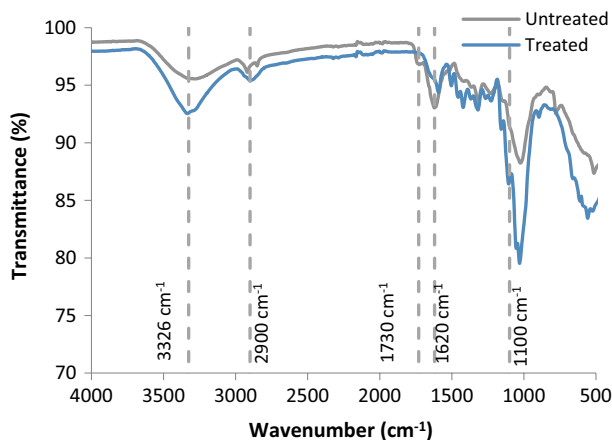


Fig. 3 FTIR spectrum for untreated and treated *Ricinus* samples



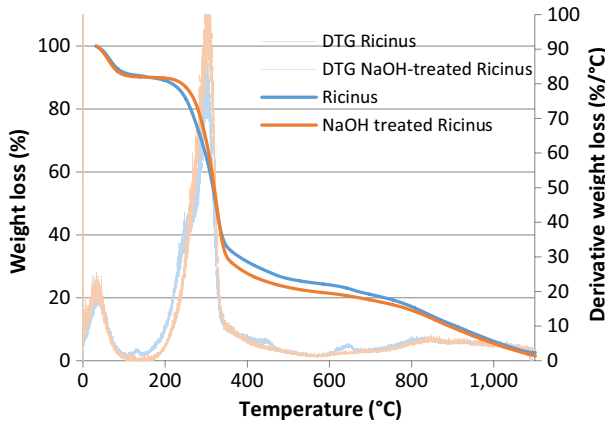


Fig. 4 Thermogravimetric (TGA) and derivative (DTG) curves for Ricinus samples

**Table 2** Degradation temperatures for *Ricinus* samples (in °C)

	Left limit	Onset	Peak
Untreated samples	227	282	333
Treated samples	252	284	333

Finally, SEM micrographs (Fig. 5) show apparent differences between samples due to the treatment. Fiber bundles of aligned fibrils can be observed for all samples, although more clearly for treated fibers. These show a rougher surface due to the removal of hemicellulose and other bonding substances, which form a layer over the bundles’ surface. On the other hand, untreated fibers show other substances (probably starch or other non-structural carbohydrates) which disappear during treatment. For treated samples, fiber walls and pit membranes are observed.

### Mechanical properties of the composite

Table 3 shows a summary of results obtained for the different properties assessed. It is observed that the density of the composites is lower than the one obtained for the pure polymer parts, being more significant than the difference for composites with treated fibers. Contrary to what was obtained in this research, other authors reported higher density for the composites with treated fibers than for those with untreated ones [15, 16]. This decrease is related to the higher porosity of composites with an increased amount of fiber or having treated fibers, as observed in wall thickness and optical microscope. This higher number of voids is also responsible for the low mechanical properties determined.

There is not much literature about the use of *Ricinus* in composites, and it mainly focuses on using epoxy resins [26–29]. Only two papers on the use of this plant in thermoplastic composites were found in the literature: one using PA11 [22], where fibers

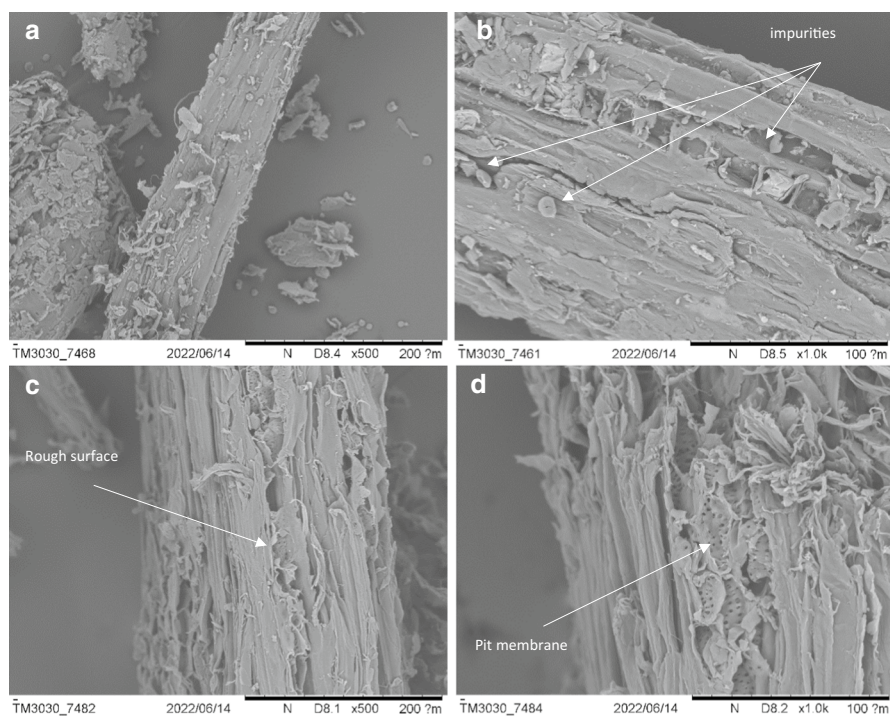


**Fig. 5** SEM pictures for **a, b** shredded material, **c, d** NaOH-treated shredded material, at  $\times 500$  and  $\times 1000$  magnifications

**Table 3** Average values ( $\pm$  standard deviations) for mechanical properties of materials

Material	Density ( $\text{g}/\text{cm}^3$ )	Impact Strength ( $\text{kJ}/\text{m}^2$ )	Tensile properties		Flexural properties	
			Strength (MPa)	Modulus (MPa)	Strength (MPa)	Modulus (MPa)
PE	$0.910 \pm 0.011$	$17.7 \pm 1.2^b$	$16.1 \pm 0.3$	$381.5 \pm 59.4^f$	$18.7 \pm 2.1^i$	$623.7 \pm 75.2^k$
PE.RC 5	$0.884 \pm 0.012$	$16.6 \pm 1.5^b$	$13.6 \pm 0.6^d$	$395.6 \pm 72.1^f$	$17.8 \pm 2.0^i$	$639.4 \pm 77.9^k$
PE.RC 10	$0.840 \pm 0.021^a$	$9.0 \pm 1.7$	$11.4 \pm 0.4^c$	$408.2 \pm 93.4^f$	$15.4 \pm 0.8^j$	$596.4 \pm 69.3^k$
PE.RCt 5	$0.855 \pm 0.009^a$	$12.1 \pm 1.3$	$13.4 \pm 0.3^d$	$589.9 \pm 64.0^g$	$17.4 \pm 1.0^i$	$676.8 \pm 137.3^k$
PE.RCt 10	$0.802 \pm 0.029$	$6.9 \pm 1.4$	$11.8 \pm 1.0^c$	$520.7 \pm 73.0^g$	$15.9 \pm 1.3^j$	$636.7 \pm 136.6^k$
PLA	$1.212 \pm 0.024$	$21.1 \pm 5.0$	$17.3 \pm 5.6$	$865.4 \pm 161.5^h$	$57.7 \pm 4.5$	$3862.1 \pm 412.1$
PLA.RC 10	$1.1272 \pm 0.025$	$3.7 \pm 0.7^c$	$23.4 \pm 3.5$	$809.3 \pm 134.8^h$	$37.6 \pm 5.0$	$3002.8 \pm 453.6$
PLA.RCt 10	$0.8641 \pm 0.100$	$2.3 \pm 0.9^c$	$10.9 \pm 4.5$	$544.4 \pm 162.5$	$21.7 \pm 5.3$	$1521.7 \pm 349.1$

Tukey tests for comparison of properties of the different series of materials have been used at a 95% confidence level. Those materials with the same superscript letter show no statistical difference for the property

helped improve the mechanical properties of laminated composites, and another using polypropylene in compression molding [24]. This last work showed better properties than those found for composites prepared similarly but using jute fibers. As rotational molding has specific features, the comparison is made for other fillers used in PE or PLA composites.

In general terms, the strength is more affected by the ratio of fibers used than for the use of NaOH to modify the fibers, even if some degradation was expected from the color and smell of obtained parts; the higher amount of fibers leads to a higher decrease in strength.

Impact properties are drastically reduced for most samples, especially for PLA ones, due to the brittle nature of this material. Only PE composites with 5% untreated fibers show no variation in impact strength compared to the matrix.

This study has obtained PLA composites with 10% of fibers with reduced flexural properties and increased tensile strength for untreated fibers, without changes in tensile modulus. Andrzejewski and collaborators have found significant decreases in tensile strength when using lower proportions of buckwheat husk [13]; this difference may be due to the use of particles with a higher L/D ratio in this research. A different work performed with 10% agave fibers led to unchanged elastic modulus and a significant decrease in tensile strength [11], although these authors were able to introduce up to 40% of fibers and get consistent parts (with poor properties in any case). The increased porosity found for treated fibers composite may explain the lower mechanical properties achieved.

The literature shows that the introduction of fillers significantly affects tensile and impact strength while modules remain unchanged or even tend to increase [12, 42]. For example, Oliveira et al. have found that using 5% hemp fibers resulted in a reduction in tensile strength and modulus higher than 50%; the use of NaOH-treated fibers allows for reducing this drop, especially for modulus [33]. Abhilash and collaborators finally found that 10% of bamboo fibers can be introduced into the PE matrix without significant decreases in mechanical properties (apart from impact strength, which is also significantly decreased) [19]. The use of *Ricinus* in the PE matrix has reduced the tensile strength, while the flexural one remains close to neat PE for 5% loadings. Different behavior happened for modules, which were kept unchanged for flexural tests and slightly increased for tensile ones in treated fiber composites. Other works in rotational molding have found lower tensile strength value and increased modulus; generally, higher loadings led to higher tensile strength drops.

It is well-known that longer fillers can lead to better mechanical properties, although the special features of rotational molding, where there is no applied pressure, limit the size of the filler to avoid entanglement and increase homogeneity. Other options to improve the mechanical behavior are using compatibilizers or obtaining parts with different layers, although these increase the process's difficulty, resulting in longer cycle times and higher costs.

## Evolution of bio-disintegration boxes

The humidity of the solid synthetic waste oscillated from 70.8% in the first week to 59.8% in week 9, ending at 61.5%. The weight of the boxes was also reduced gradually, due mainly to water evaporation. The starting pH was 8.3, increased to a maximum of 9.1 in week 4, then decreased again to reach values around 8.0; during these first weeks, boxes smelled ammonia. At the end of the assay, the bio-waste did not have any specific odor, and its color was notably darker.

The temperature inside the bio-waste was progressively decreasing; this assay took place during winter, and the room temperature was also relatively low. In any case, the internal temperature was above room temperature, at least 3 °C, with signs of humidity evaporation, which can be considered a result of existing biological activity, even if this was low. After the assay, PLA-composite samples were recovered broken.

The bio-disintegration degree was calculated as the percentage of weight lost, that is, the difference in weight of the dry mass for each test bar at the beginning of the end of the assay divided by the initial sample weight. After recovering the samples from the assay, these were dried and weighed. Table 4 shows the weight loss values for the different pieces and humidity absorption before and after the disintegration assay.

It can be observed that PE samples have almost no change, although after the assay the samples tend to absorb more moisture. Neat PLA samples suffer virtually no weight loss while also increasing hydrophilicity. Most significant differences are observed for PLA-composites, reaching up to 5% of weight loss and multiplying by over 30 the amount of moisture absorption. It can then be concluded that using vegetal fibers increases the capacity of the material to absorb water, which is a crucial step for PLA degradation [43, 44]. Humidity absorption is also increased for PE composites, although no weight loss was aroused, which was expected. At this point, it is interesting to note that, although PLA is usually considered a biodegradable material, it is only utterly valid under certain conditions, typically involving high temperatures (around 58 °C) [45, 46]. Some works proposed using mesophilic conditions, closer to the assay shown in this paper [47], as usually municipal waste treatment plants operate in these conditions (around 37 °C) and have lower energy

**Table 4** Weight loss and humidity absorption for rotomolded samples (in %)

	Weight loss (%)	Humidity absorption (%)	
		Before	After
PE	0.11 ± 0.03	0.09 ± 0.03	0.86 ± 0.31
PE + 10% <i>Ricinus</i>	0.43 ± 0.07	1.11 ± 0.06	8.63 ± 0.93
PE + 10% treated <i>Ricinus</i>	0.26 ± 0.01	1.07 ± 0.08	6.74 ± 0.37
PLA	0.30 ± 0.10	0.68 ± 0.03	4.03 ± 0.55
PLA + 10% <i>Ricinus</i>	4.89 ± 2.22	1.38 ± 0.05	23.91 ± 1.16
PLA + 10% treated <i>Ricinus</i>	3.52 ± 1.52	1.48 ± 0.05	38.37 ± 2.22

requirements; weight losses obtained for PLA in these conditions are close to those obtained in this research [44]. Crystallinity, molecular weight, and L/D monomer ratio also greatly influence the degradation properties of PLA; in general terms, the higher crystallinity, the lower the degradation rates. The PLA grade used in this research contains 99% L-isomer, which contributes to higher crystallinity and lower degradation kinetics [48].

## Microscopic observations

Some voids were observed in the composite parts, especially in those with treated fibers, even before the bio-disintegration assay. As commented above, wall thickness for these parts was higher (and so lower is density). Fibers are well distributed in the matrix (Fig. 6) and on all the sides of the molded parts. Regarding the changes observed due to the biological process, PE parts do not show any significant modification, apart from the darkening of the part. For PLA, some small cracks can be observed on the parts' surfaces, while the composite samples are plenty on the surface and in cross sections. The fibers' water uptake may have forced the cracks to appear, just by fibers swelling or by the water effect in the PLA and the start of hydrolysis.

The cracks appearing in PLA composite parts (Fig. 6e, f, h) were visible to the naked eye just when recovering the pieces from the synthetic compost, and some were even broken after the process. Even for the low weight loss observed in the assay, the degradation is evident in these samples.

The SEM micrographs for PE and PLA samples show a smooth surface, almost free of porosity, while for composites, some voids can be found (Figs. 7, 8, respectively). For both matrixes, fibers appear randomly distributed, and some lack of material is observed in the treated *Ricinus* samples, thus explaining the relatively poor mechanical properties of the composite. For PLA samples, the material appears fragmented, with many cracks on all surfaces of PLA-composite parts, as also observed by optical microscopy.

## DSC

Typical DSC curves and results are obtained for all composites before and after the disintegration assay (Fig. 9); results are summarized in Table 5 for PE samples and Table 6 for PLA ones.

For polyethylene samples, the melting temperature is around 129 °C, with no difference due to the fibers' introduction, either untreated or treated. No differences between the two heating cycles were found. No difference in the temperatures due to the bio-disintegration assay was found, confirming that the biological process does not modify these materials. Besides, the melting and crystallization temperatures remain unchanged, and the enthalpies are just slightly reduced due to fibers' introduction. Composites samples show lower crystallinity values than neat matrixes. Other authors have found similar behavior, with almost unchanged thermal

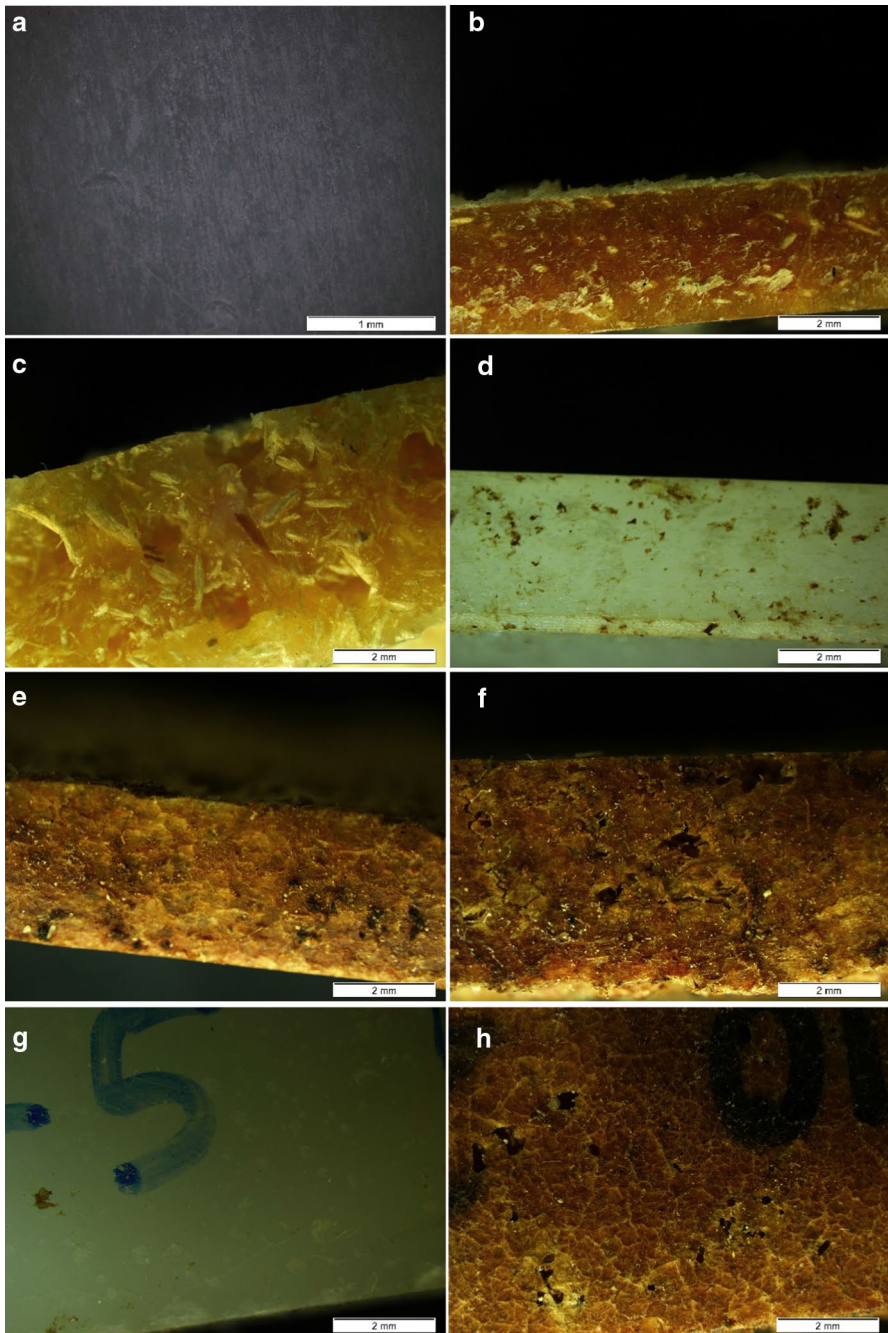


**Fig. 6** Lateral view of PLA samples, before the disintegration assay: **a** Neat PLA, **b** 10% *Ricinus*, **c** 10% treated *Ricinus*, and after the assay, **d** PLA, **e** 10% *Ricinus*, **f** 10% treated *Ricinus*, **g** surface of PLA, **h** surface of 10% *Ricinus* PLA

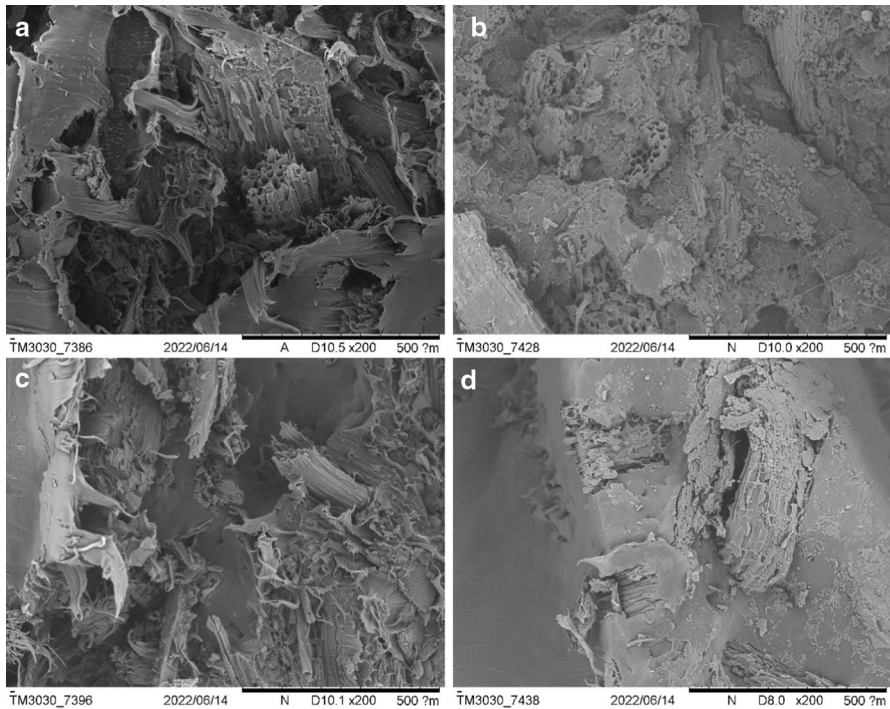


**Fig. 7** SEM micrographs for PE samples; left pictures correspond to samples before disintegration assay, right ones, after. **a, b** PE + 10% *Ricinus* fibers, **c, d** PE + 10% treated *Ricinus* fibers

properties due to the incorporation of dissimilar materials, with crystallinity values around 40% for PE [13].

For PLA samples, the glass transition (58 °C) and melting temperatures (170 °C) are placed within the ranges indicated by the product datasheet and are similar to other PLA-based materials. The  $T_g$  increases with the introduction of the castor oil material, as this may hinder the mobility of PLA chains [11]. The similar (higher in fact) value for  $T_m$  found for composites may indicate that the PLA matrix had not suffered any degradation during the rotomolding process. Due to the PLA grade used in this research, crystallinity values for PLA are significantly higher than those achieved in other works [13]. On the other hand, the crystallization peak in the cooling stage appears in all samples, contrary to what was observed in [13]. Greco and collaborators [3] have found that rotomolded PLA does not show any cold crystallization peak after aging for 60 days at room temperature. This is in line with observations in this study, where DSC was not performed immediately after parts obtaining. There is not a clear trend on the effect of *Ricinus* in the material crystallinity; apparently, this tends to decrease for the untreated filler, while it is similar for the treated one.

Finally, PLA samples show significant changes in the thermal behavior because of the bio-disintegration assay. After the biological assay, the composites' melting and glass transition temperatures are decreased by around 10%. This may show a

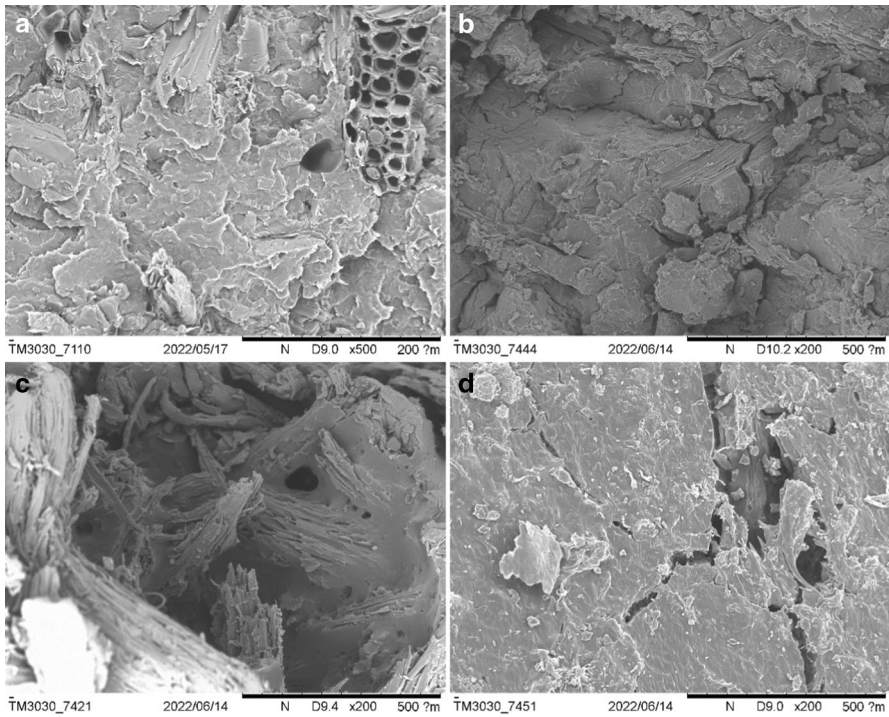


**Fig. 8** SEM micrographs for PLA composite samples; left pictures correspond to samples before disintegration assay, right ones after. **a, b** PLA + 10% *Ricinus* fibers, **c, d** PLA + 10% treated *Ricinus* fibers

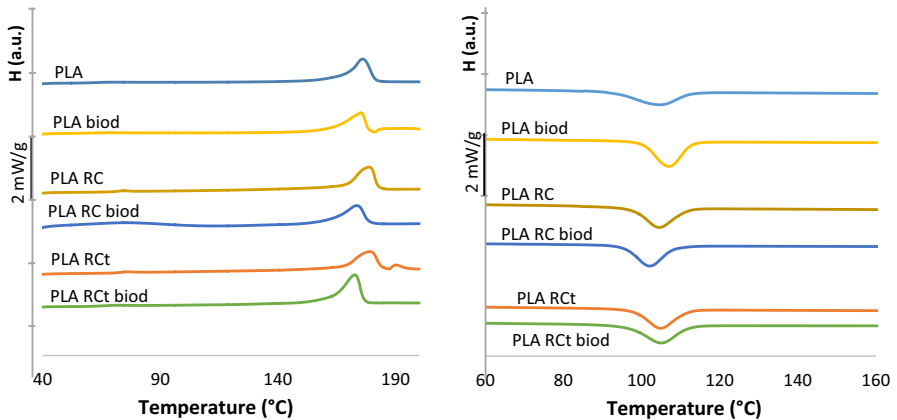


**Fig. 9** DSC curves for PLA samples before and after the disintegration assay for the first heating (left) and the cooling (right) cycles



**Table 5** Thermal parameters for PE samples from DSC assays

Material	$T_{m1}$ (°C)	$T_{m2}$ (°C)	$T_C$ (°C)	$\chi_1$ (%)	$\chi_2$ (%)
<i>Before the disintegration assay</i>					
PE	129.0±0.5	127.0±0.1	109.9±0.2	41.4±0.8	38.2±1.6
PE.RC 10%	129.6±0.3	127.3±0.8	109.7±1.1	37.8±3.5	33.2±2.1
PE.RCt 10%	129.1±0.1	129.6±0.3	128.3±0.4	30.5±3.8	28.8±4.9
<i>After the disintegration assay</i>					
PE	129.3±0.9	128.5±0.8	108.5±0.7	30.6±2.5	30.2±5.1
PE.RC 10%	129.2±0.7	128.1±0.8	108.6±1.0	37.1±3.1	33.2±4.7
PE.RCt 10%	129.2±1.1	127.8±0.4	109.1±0.4	28.4±4.4	27.9±4.2

**Table 6** Thermal parameters for PLA samples from DSC assays

Material	$T_{m1}$ (°C)	$T_{m2}$ (°C)	$T_C$ (°C)	$\chi_1$ (%)	$\chi_2$ (%)	$T_g$ (°C)
<i>Before the disintegration assay</i>						
PLA	170.4±1.4	167.3±3.0	109.0±0.4	61.9±5.5	52.1±10.8	58.1±0.7
PLA.RC	175.2±1.5	175.0±0.9	109.2±0.5	48.4±2.0	49.6±5.8	67.8±1.0
PLA.RCt	176.1±2.1	176.1±0.5	109.2±0.2	58.7±12.1	55.8±9.4	68.8±0.5
<i>After the disintegration assay</i>						
PLA	168.5±1.8	163.1±2.5	107.2±3.6	57.7±12.3	48.0±9.0	59.1±2.8
PLA.RC	167.6±1.1	164.1±3.7	104.2±2.1	54.8±4.3	52.0±5.2	59.6±0.2
PLA.RCt	160.7±3.8	146.0±6.6	89.9±10.4	70.2±1.1	46.9±3.8	61.4±3.5

reduction in the average molecular weight of the polymer and, thus, that the assay degrades to some extent the matrix.

**FTIR**

FTIR spectra for the composite samples with PE or PLA matrix do not show any significant differences due to the fiber introduction (only the disappearance of a peak at around 1646  $\text{cm}^{-1}$ , which could be related to moisture). This is mainly due to the polymer entirely covering the fibers. No differences can be observed in spectra for PE samples before and after the bio-disintegration assay (data not shown), confirming, once again, that the introduction of the *Ricinus* in the PE does not affect the degradability of the matrix, as otherwise expected.

Finally, the spectra for PLA show some differences due to the bio-disintegration process. These spectra show the typical bands for PLA, being the bands related to carbonyl and ester groups of particular interest for this study because the degradation of the matrix can lead to the formation of anhydrides, carbonyl, and carboxyl groups. So, Fig. 10 shows the spectra in the region of interesting peaks for PLA,

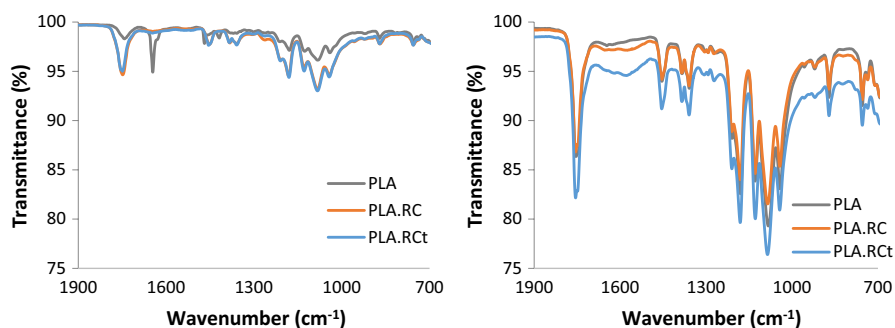


**Fig. 10** FTIR spectra for PLA samples before the disintegration assay (left) and after (right)

namely between 1900 and 700  $\text{cm}^{-1}$ , looking at the bands at 1749  $\text{cm}^{-1}$  ( $-\text{C}=\text{O}$  stretch in lactide) and at 1180, 1078, and 1043  $\text{cm}^{-1}$  ( $\text{C}-\text{O}$  stretch).

No important differences are observed among the three materials series, especially after the bio-disintegration assay. The material is then modified to the same extent, independently of having fibers or not. Only some bands seem slightly more intense compared to the baseline, which could be related to a greater degree of the modifications in the material.

## Conclusions

*Ricinus communis* stems have been characterized to determine their chemical composition, thermal stability, and morphology. The results show that this material could be potentially used as a filler in thermoplastic matrices, which has not been explored in the literature.

The milled material has been introduced in PE and PLA matrixes, obtaining good fiber distribution for all composites. A simple dry blending method could not be the optimal way to pre-process this material if higher filler ratios were to be used. In any case, composites with up to 10% *Ricinus* with good aesthetics were obtained. Treated fibers produced thicker walls with higher porosity, which explains the poor mechanical properties; untreated fibers gave more compact and darker parts.

Impact properties are significantly affected for both matrixes due to the introduction of *Ricinus* particles, except for 5% PE composites. Tensile strength is reduced for all PE composites, especially for 10% loadings; the treated fibers provided a higher elastic modulus than the untreated ones, and then pure PE parts. Flexural behavior is not modified for 5% PE composites. In the case of PLA, 10% composites provide higher tensile strength and similar elastic modulus to pure PLA, with reduced flexural properties. Treated fibers decreased tensile and flexural properties by half than neat PLA due to the high number of voids found in these parts, as observed in optical and electronic microscopes.

The bio-disintegration assay does not deteriorate PE composites, while the PLA ones are considerably modified. In these last samples, the introduction of *Ricinus*

particles has significant influence, as composite specimens show more profound modifications than PLA ones. For example, composite test bars were broken during the assay, while PLA ones only showed some surface cracks. This degradation is not visible on FTIR analysis, although clear on DSC tests, with a significant decrease in glass transition and melting temperatures.

**Acknowledgements** European Funding for Regional Development (FEDER) funded this research, providing funds for the MAC Inv2Mac project (Grant Number MAC2/4.6d/229) through the INTERREG MAC 2014–2020 program. Luis Suárez also acknowledges the funding through the Ph.D. grant program cofinanced by the Canarian Agency for Research, Innovation and Information Society of the Canary Islands Regional Council for Employment, Industry, Commerce and Knowledge (ACIISI) and by the European Social Fund (ESF) (Grant Number TESIS2021010008).

**Author contributions** ZO, LS and MDM performed the study conception and design. Material preparation, data collection and analysis were performed by LS, FR, JC, ANB and ZO. ZO wrote the first draft of the manuscript, and all authors commented on previous versions. All authors read and approved the final manuscript.

**Funding** Open Access funding provided thanks to the CRUE-CSIC agreement with Springer Nature. The research is part of the MAC Inv2Mac project (Grant Number MAC2/4.6d/229), funded by the European Funding for Regional Development (FEDER) through the INTERREG MAC 2014–2020 program.

**Data availability** The datasets generated during the current study are available from the corresponding author on reasonable request.

## Declarations

**Conflict of interest** The authors report there are no competing interests to declare.

**Open Access** This article is licensed under a Creative Commons Attribution 4.0 International License, which permits use, sharing, adaptation, distribution and reproduction in any medium or format, as long as you give appropriate credit to the original author(s) and the source, provide a link to the Creative Commons licence, and indicate if changes were made. The images or other third party material in this article are included in the article's Creative Commons licence, unless indicated otherwise in a credit line to the material. If material is not included in the article's Creative Commons licence and your intended use is not permitted by statutory regulation or exceeds the permitted use, you will need to obtain permission directly from the copyright holder. To view a copy of this licence, visit <http://creativecommons.org/licenses/by/4.0/>.

## References

1. Hejna A, Barczewski M, Andrzejewski J et al (2020) Rotational molding of linear low-density polyethylene composites filled with wheat bran. *Polymers (Basel)* 12:1004. <https://doi.org/10.3390/POLYM12051004>
2. Barczewski M, Hejna A, Aniśko J et al (2022) Rotational molding of polylactide (PLA) composites filled with copper slag as a waste filler from metallurgical industry. *Polym Test* 106:107449. <https://doi.org/10.1016/J.POLYMERTESTING.2021.107449>
3. Greco A, Ferrari F, Maffezzoli A (2019) Processing of super tough plasticized PLA by rotational molding. *Adv Polym Technol* 2019:1–8. <https://doi.org/10.1155/2019/3835829>
4. Ruiz-Silva E, Rodríguez-Ortega M, Rosales-Rivera LC et al (2021) Rotational molding of poly(lactic acid)/polyethylene blends: effects of the mixing strategy on the physical and mechanical properties. *Polymers* 13:217. <https://doi.org/10.3390/POLYM13020217>
5. Greco A, Maffezzoli A (2017) Rotational molding of poly(lactic acid): effect of polymer grade and granulometry. *Adv Polym Technol* 36:477–482. <https://doi.org/10.1002/ADV.21630>

6. González-López ME, Pérez-Fonseca AA, Cisneros-López EO et al (2019) Effect of maleated PLA on the properties of rotomolded PLA-agave fiber biocomposites. *J Polym Environ* 27:61–73. <https://doi.org/10.1007/s10924-018-1308-2>
7. Pick L, Hanna PR, Gorman L (2022) Assessment of processibility and properties of raw post-consumer waste polyethylene in the rotational moulding process. *J Polym Eng* 42:374–383. <https://doi.org/10.1515/POLYENG-2021-0212/MACHINEREADABLECITATION/RIS>
8. Aniśko J, Barczewski M, Mielniński P et al (2022) Valorization of disposable polylactide (PLA) cups by rotational molding technology: The influence of pre-processing grinding and thermal treatment. *Polym Testing* 107:107481. <https://doi.org/10.1016/j.polymertesting.2022.107481>
9. Wang B, Panigrahi S, Tabil L, Crerar W (2007) Pre-treatment of flax fibers for use in rotationally molded biocomposites. *J Reinf Plast Compos* 26:447–463. <https://doi.org/10.1177/0731684406072526>
10. Torres FG, Aragon CL (2006) Final product testing of rotational moulded natural fibre-reinforced polyethylene. *Polym Test* 25:568–577. <https://doi.org/10.1016/j.polymertesting.2006.03.010>
11. Cisneros-López EO, Pérez-Fonseca AA, González-García Y et al (2018) Polylactic acid–agave fiber biocomposites produced by rotational molding: a comparative study with compression molding. *Adv Polym Technol* 37:2528–2540. <https://doi.org/10.1002/ADV.21928>
12. León LDVE, Escocio VA, Visconte LLY et al (2020) Rotomolding and polyethylene composites with rotomolded lignocellulosic materials: a review. *J Reinf Plast Compos* 39:459–472. <https://doi.org/10.1177/0731684420916529>
13. Andrzejewski J, Krawczak A, Wesoły K, Szostak M (2020) Rotational molding of biocomposites with addition of buckwheat husk filler. Structure–property correlation assessment for materials based on polyethylene (PE) and poly(lactic acid) PLA. *Compos Part B Eng* 202:108410. <https://doi.org/10.1016/j.compositesb.2020.108410>
14. Cisneros-López EO, González-López ME, Pérez-Fonseca AA et al (2017) Effect of fiber content and surface treatment on the mechanical properties of natural fiber composites produced by rotomolding. *Compos Interfaces* 24:35–53. <https://doi.org/10.1080/09276440.2016.1184556>
15. Hanana FE, Rodrigue D (2021) Effect of particle size, fiber content, and surface treatment on the mechanical properties of maple-reinforced LLDPE produced by rotational molding. *Polym Polym Compos* 29:343–353. <https://doi.org/10.1177/0967391120916602>
16. Ortega Z, Romero F, Paz R et al (2021) Valorization of invasive plants from macaronesia as filler materials in the production of natural fiber composites by rotational molding. *Polymers* 13:2220. <https://doi.org/10.3390/POLYM13132220>
17. Robledo-Ortíz JR, González-López ME, Martín del Campo AS et al (2020) Fiber-matrix interface improvement via glycidyl methacrylate compatibilization for rotomolded poly(lactic acid)/agave fiber biocomposites. *J Compos Mater* 55:201–212. <https://doi.org/10.1177/0021998320946821>
18. Ortega Z, Monzón MD, Benítez AN et al (2013) Banana and abaca fiber-reinforced plastic composites obtained by rotational molding process. *Mater Manuf Process* 28:879–883. <https://doi.org/10.1080/10426914.2013.792431>
19. Abhilash SS, Singaravelu DL (2020) Effect of fiber content on mechanical and morphological properties of bamboo fiber-reinforced linear low-density polyethylene processed by rotational molding. *Trans Indian Inst Met* 73:1549–1554. <https://doi.org/10.1007/s12666-020-01922-y>
20. Suárez L, Castellano J, Romero F et al (2021) Environmental hazards of giant reed (*Arundo donax* L.) in the macaronesia region and its characterisation as a potential source for the production of natural fibre composites. *Polymers (Basel)* 13:2101. <https://doi.org/10.3390/POLYM13132101>
21. Díaz S, Ortega Z, McCourt M et al (2018) Recycling of polymeric fraction of cable waste by rotational moulding. *Waste Manag* 76:199–206. <https://doi.org/10.1016/j.wasman.2018.03.020>
22. Heitzmann MT, Veidt M, Ng CT et al (2013) Single-plant biocomposite from *Ricinus communis*: preparation, properties and environmental performance. *J Polym Environ* 21:366–374. <https://doi.org/10.1007/s10924-012-0517-3>
23. Rocha MCG, de Acevedo NIA, de Oliveira CIR et al (2021) Mercerization effect on the properties of LDPE/PHB composites reinforced with castor cake. *Polímeros*. <https://doi.org/10.1590/0104-1428.07720>
24. Vinayaka DL, Vijaykumar G, Madhavi D et al (2017) *Ricinus communis* plant residues as a source for natural cellulose fibers potentially exploitable in polymer composites. *Ind Crops Prod* 100:126–131. <https://doi.org/10.1016/j.indcrop.2017.02.019>

25. Nijandhan K, Muralikannan R, Venkatchalam S (2018) *Ricinus communis* fiber as potential reinforcement for lightweight polymer composites. *Mater Res Express* 5:095307. <https://doi.org/10.1088/2053-1591/aad617>
26. Egala R, Jagadeesh GV, Setti SG (2021) Experimental investigation and prediction of tribological behavior of unidirectional short castor oil fiber reinforced epoxy composites. *Friction* 9:250–272. <https://doi.org/10.1007/S40544-019-0332-0>
27. Egala R, Setti SG (2021) Influence of surface modifications of Castor oil fibre on mechanical properties of fibre reinforced Epoxy composites. *Adv Mater Process Technol.* <https://doi.org/10.1080/2374068X.2021.1959107>
28. Egala R, Gangi Setti S (2018) Impact characterization of epoxy LY556/*Ricinus communis* L plant natural fiber composite materials. *Mater Today Proc* 5:26799–26803. <https://doi.org/10.1016/J.MATPR.2018.08.159>
29. Egala R, Setti G (2018) Effect of short and randomly oriented *Ricinus communis* L (castor oil) plant on mechanical behaviour of *Ricinus communis* L/epoxy LY556 composites. *Mater Today Proc* 5:8065–8072
30. American National Standard Institute (1977) ANSI/ASTM, 1977a. Standard test. Methods for Lignin in Wood—D 1106-56. Washington DC, USA
31. Browning B (1967) Methods of wood chemistry, vol I and II. Interscience Publishers, New York
32. American National Standard Institute (1977) ANSI/ASTM, 1977b. Standard test methods for alpha-cellulose in wood D 1103-60. Washington DC, USA
33. Oliveira MAS, Pickering KL, Sunny T, Lin RJT (2021) Treatment of hemp fibres for use in rotational moulding. *J Polym Res* 28:3. <https://doi.org/10.1007/s10965-021-02414-3>
34. Shah AA, Hasan F, Hameed A, Ahmed S (2008) Biological degradation of plastics: a comprehensive review. *Biotechnol Adv* 26:246–265
35. Grigoriou AH, Ntalos GA (2001) The potential use of *Ricinus communis* L. (Castor) stalks as a lignocellulosic resource for particleboards. *Ind Crops Prod* 13:209–218. [https://doi.org/10.1016/S0926-6690\(00\)00078-9](https://doi.org/10.1016/S0926-6690(00)00078-9)
36. Li X, Du G, Wang S, Yu G (2014) Physical and mechanical characterization of fiber cell wall in castor (*Ricinus communis* L.) stalk. *BioResources* 9:1596–1605. <https://doi.org/10.15376/biores.9.1.1596-1605>
37. Chikouche MDL, Merrouche A, Azizi A et al (2015) Influence of alkali treatment on the mechanical properties of new cane fibre/polyester composites. *J Reinf Plast Compos* 34:1329–1339. <https://doi.org/10.1177/0731684415591093>
38. Bessa W, Trache D, Derradji M et al (2020) Characterization of raw and treated *Arundo donax* L. cellulosic fibers and their effect on the curing kinetics of bisphenol A-based benzoxazine. *Int J Biol Macromol* 164:2931–2943. <https://doi.org/10.1016/j.ijbiomac.2020.08.179>
39. Scalici T, Fiore V, Valenza A (2016) Effect of plasma treatment on the properties of *Arundo donax* L. leaf fibres and its bio-based epoxy composites: a preliminary study. *Compos B Eng* 94:167–175. <https://doi.org/10.1016/j.compositesb.2016.03.053>
40. Martínez-Sanz M, Erboz E, Fontes C, López-Rubio A (2018) Valorization of *Arundo donax* for the production of high performance lignocellulosic films. *Carbohydr Polym* 199:276–285. <https://doi.org/10.1016/j.carbpol.2018.07.029>
41. Fiore V, Scalici T, Valenza A (2014) Characterization of a new natural fiber from *Arundo donax* L. as potential reinforcement of polymer composites. *Carbohydr Polym* 106:77–83. <https://doi.org/10.1016/j.carbpol.2014.02.016>
42. Höfler G, Lin RJT, Jayaraman K (2018) Rotational moulding and mechanical characterisation of halloysite reinforced polyethylenes. *J Polym Res.* <https://doi.org/10.1007/s10965-018-1525-3>
43. Moliner C, Finocchio E, Arato E et al (2020) Influence of the degradation medium on water uptake, morphology, and chemical structure of poly(lactic acid)-sisal bio-composites. *Materials* 13:3974. <https://doi.org/10.3390/ma13183974>
44. Bayerl T, Geith M, Somashekar AA, Bhattacharyya D (2014) Influence of fibre architecture on the biodegradability of FLAX/PLA composites. *Int Biodeterior Biodegrad* 96:18–25. <https://doi.org/10.1016/j.ibiod.2014.08.005>
45. Ruggero F, Belardi S, Caretti E et al (2021) Rigid and film bioplastics degradation under suboptimal composting conditions: a kinetic study. *Waste Manag Res.* <https://doi.org/10.1177/0734242X211063731>

46. Boonmee C, Kositanont C, Leejarkpai T (2022) Degradation behavior of biodegradable plastics in thermophilic landfill soil and wastewater sludge conditions. *Environ Res Eng Manag* 78:57–69. <https://doi.org/10.5755/J01.EREM.78.1.29502>
47. Cucina M, De Nisi P, Trombino L et al (2021) Degradation of bioplastics in organic waste by mesophilic anaerobic digestion, composting and soil incubation. *Waste Manag* 134:67–77. <https://doi.org/10.1016/J.WASMAN.2021.08.016>
48. Gorrasi G, Pantani R (2013) Effect of PLA grades and morphologies on hydrolytic degradation at composting temperature: assessment of structural modification and kinetic parameters. *Polym Degrad Stab* 98:1006–1014. <https://doi.org/10.1016/J.POLYMDEGRADSTAB.2013.02.005>

**Publisher's Note** Springer Nature remains neutral with regard to jurisdictional claims in published maps and institutional affiliations.